

# Interband tunneling in narrow-gap heterostructures

F. T. Vas'ko

*Institute of Semiconductors, Ukrainian SSR Academy of Sciences*

(Submitted 18 February 1991)

Zh. Eksp. Teor. Fiz. **100**, 635–646 (August 1991)

We calculate the contribution to the total tunneling current through a barrier due to interband tunneling, in which electron-hole pairs appear at the barrier whose constituents are on opposite sides of the barrier layer. This process switches on when a potential difference larger than  $\varepsilon_g/|e|$  is applied to a tunneling structure consisting of two layers of narrow-gap doped semiconductor (where  $\varepsilon_g$  is the width of the forbidden band of the semiconductor) with a wide-gap semiconductor barrier between them. We find numerical estimates of the electron-hole pair concentration generated at such a barrier for heterostructures based on lead chalcogenides. In addition to serving as IR radiators, these tunneling structures are also interesting sources of negative resistance.

## 1. INTRODUCTION

Ordinary tunneling processes in metal-insulator-metal structures or semiconductor heterostructures<sup>1,2</sup> do not involve transitions in which the band state label of a current carrier changes. However, for tunneling heterostructures consisting of two layers of narrow-gap doped semiconductor ( $\varepsilon_g$  is the width of the forbidden band of the semiconductor) separated by a wide-gap semiconductor barrier occupying the region  $|z| < d/2$ , application of a potential difference  $V > \varepsilon_g/|e|$  can lead to a fundamental change in the physics involving the switching-on of a channel for interband tunneling<sup>1)</sup>, i.e., to the generation of electron-hole pairs at the boundaries  $z = \pm d/2$  of the barrier. For definiteness, we will treat the case where the voltage decreases across the barrier from left to right (see the band diagram in Fig. 1), so that the process of interband tunneling transfers electrons from states of the valence band to the conduction band. This process is allowed for energies  $E$  lying in the interval bounded by the inequality

$$(|e|V - \varepsilon_g)/2 > E > (\varepsilon_g - |e|V)/2,$$

whereas tunneling between conduction band (or valence band) states corresponds to the energy interval

$$|E| > (\varepsilon_g + |e|V)/2.$$

However, the first of these inequalities is not a sufficient condition for switching on interband tunneling: the threshold voltage also depends on the way the narrow-gap semiconductors are doped. It is clear from the band diagrams for  $n$ - and  $p$ -type heterostructures shown in Fig. 1 (where  $\mu_e$  and  $\mu_h$  are the appropriate Fermi levels) that these processes actually switch on when  $|e|V > \varepsilon_g + \mu$ . For  $|e|V - \varepsilon_g \ll \varepsilon_g$  the interband contribution to the current is due to transitions between low-energy valence- and conduction-band states; in this approximation we can derive simple analytic dependences for the tunneling current.

The tunneling current calculations described here are based on a symmetric two-band (Dirac-like) model of the energy spectrum. The case of an isotropic spectrum and heterostructure band offsets that are large compared to  $\varepsilon_g$  describes tunneling between equivalent pairs of valleys in heterostructures based on lead chalcogenides (we assume that mixing of states from different valleys by the sharp hetero-

structure potential is small).<sup>4</sup> In addition to these approximations, in investigating the band diagram of Fig. 1 we also assume that all the applied voltage  $V$  falls at the barrier (i.e., the case of flat bands in the strongly doped  $n$ - and  $p$ -type materials), and that the band offsets  $\Delta E_{c,v}$  are much larger than  $|e|V$ , so that the positions of the band extrema in the barrier may be considered constant (see the dotted lines on Figs. 1b and 1c). Although this latter approximation results in a rather crude picture of the IV characteristics of the structure, it is convenient for estimating the concentration of electron-hole pairs generated by the barrier.

The simple analytic expressions which follow from these approximations show the qualitative differences between this case and that of Zener tunneling in a reverse-biased  $pn$ -junction. In our structure the character of the below-barrier motion is different (here the process of tunneling takes place far below the barrier, which decreases the overall magnitude of the current); furthermore, the width of the tunneling layer does not depend on the applied voltage (whereas in a  $pn$ -junction the thickness of the depletion layer increases with increasing  $V$ , which also decreases the tunneling current). We also note that the interband tunneling current turns out to be a strong function of the ratio  $\Delta E_c/\Delta E_v \equiv \alpha^2$ ; in the limit  $\Delta E_v = 0$  (for which the variation in the positions of the valence band extrema corresponds to

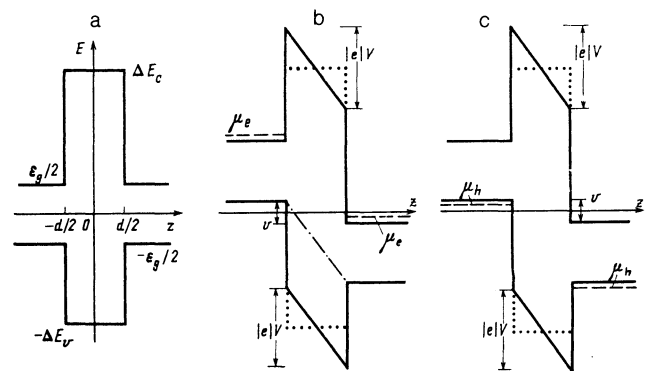


FIG. 1. Band diagram of heterostructures under discussion. a) for zero potential difference applied to the structure, b) for a voltage  $|e|V > \varepsilon_g$  across an  $n$ -type structure, c) for a  $p$ -type structure under the same conditions. The dashed lines denote the Fermi level, and the dotted lines approximate the positions of the band extrema in the barrier.

the dotted-dashed line on the band diagram Fig. 1b) this current increases rapidly. We emphasize that for tunneling through a high barrier ( $\Delta E_{c,v} \gg \varepsilon_g$ ) there are qualitative differences even for the case  $|e|V < \varepsilon_g$ , in that the transparency of the barrier during tunneling between low energy conduction- or valence-band states depends (in contrast to the usual quantum mechanical formula<sup>5</sup>) on the parameter  $\alpha$ .

Below in Sec. 2 we discuss the quantum mechanics of electron tunneling in a structure made of narrow-gap semiconductors separated by a wide-gap barrier. Then in Sec. 3 we calculate the transmission coefficient which corresponds to the process of interband tunneling and whose value determines its contribution to the tunneling current. Following this (Secs. 4 and 5), we discuss the increase in the interband tunneling for the case  $\Delta E_v = 0$  and the intraband contribution to the tunneling current. In the concluding Sec. 6, we give an estimate for the concentration of electron-hole pairs generated by a wide-gap barrier and discuss the approximations used.

## 2. DESCRIPTION OF SCATTERING BY A WIDE-GAP BARRIER (THE TWO-BAND HETEROSTRUCTURE MODEL)

The dynamics of low-energy electronic states (i.e., close to the extrema of the conduction or valence bands) are determined within the  $\mathbf{k} \cdot \mathbf{p}$  approximation by the  $4 \times 4$  Hamiltonian matrix

$$\hat{h} = \hat{\varepsilon}(z) + s \begin{vmatrix} 0 & I \\ I & 0 \end{vmatrix} (\boldsymbol{\sigma} \mathbf{P}) \equiv \hat{\varepsilon}(z) + \hat{\mathbf{V}} \mathbf{P}, \quad (1)$$

in which  $\mathbf{P} = (\mathbf{p}, -i\hbar \cdot d/dz)$  is the momentum operator; the characteristic interband velocity  $s$  and Pauli matrices  $\boldsymbol{\sigma}$  define the velocity operator  $\hat{\mathbf{v}}$  entering into the right-hand side of the equation. Since we are investigating the case of symmetric bands, terms that are quadratic in  $\mathbf{P}$  have been neglected in Eq. (1). The diagonal matrix  $\hat{\varepsilon}(z)$ , which depends on the transverse coordinate  $z$ , is defined by the position of the spin-degenerate extrema of the conduction and valence bands  $\varepsilon_{c,v}(z)$ . For the case of strongly doped narrow-gap materials the bias voltage  $V$  falls across the tunnel barrier, which occupies the region  $|z| < d/2$ , so that the band diagrams in Figs. 1b and 1c correspond to the expressions

$$\varepsilon_c(z) = \begin{cases} (\varepsilon_g + |e|V)/2, & z < -d/2, \\ \Delta E_c - |e|Vz/d, & |z| < d/2, \\ (\varepsilon_g - |e|V)/2, & z > d/2, \end{cases} \quad (2)$$

$$\varepsilon_v(z) = \begin{cases} (|e|V - \varepsilon_g)/2, & z < -d/2 \\ -\Delta E_v - |e|Vz/d, & |z| < d/2, \\ -(|e|V + \varepsilon_g)/2, & z > d/2. \end{cases} \quad (2)$$

Using the resulting four-component wave function  $\psi(z)$  of a state with energy  $E$  [which is determined by the Schrodinger equation  $\hat{h}\psi(z) = E\psi(z)$ ] we obtain the  $z$  component of the current density

$$j = \psi(z)^+ \hat{v}_z \psi(z); \quad (3)$$

for the one-dimensionally nonuniform system under discussion here the current  $j$  does not depend on  $z$ . The equation  $dj/dz = 0$  can be verified by using the Schrodinger equation given above and the Hermitian character of the Hamiltonian  $\hat{h}$ .

In investigating the problem of scattering by a barrier, it is convenient to carry out a unitary transformation which diagonalizes the Hamiltonian (1) in the spin variables (see, e.g., Ref. 6), so that the four-component spinor  $\psi(z)$  is given in the new representation by the expression

$$\begin{pmatrix} \varphi \\ \chi \end{pmatrix} |\sigma\rangle.$$

Here  $|\sigma\rangle$  is an eigenfunction of  $\sigma_z$  ( $\sigma = \pm 1$  are the spin projections on the axis perpendicular to the  $2-D$  momentum  $\mathbf{p}$ , where the latter describes the motion along the barrier); for the wave function components  $\varphi$  and  $\chi$  we obtain a system of first-order equations

$$\begin{aligned} [\varepsilon_c(z) - E] \varphi + s \left( \sigma p + \hbar \frac{d}{dz} \right) \chi &= 0, \\ s \left( \sigma p - \hbar \frac{d}{dz} \right) \varphi + [\varepsilon_v(z) - E] \chi &= 0, \end{aligned} \quad (4)$$

in which  $p = |\mathbf{p}|$ , and the position of the extrema  $\varepsilon_{c,v}$  is determined by (2). After this unitary transformation, the  $z$ -component of the current density defined in (3) for a state characterized by energy  $E$  and quantum numbers  $\mathbf{p}, \sigma$  is given by the expression

$$j|_{E,\sigma,\mathbf{p}} = is(\varphi^* \chi - \chi^* \varphi). \quad (5)$$

In solving the system (4) it is convenient to eliminate the barrier region from consideration by connecting the wave functions on the left-hand half-space ( $z < -d/2$ )

$$\begin{pmatrix} \varphi^l \\ \chi^l \end{pmatrix}$$

with those on the right-hand half-space ( $z > d/2$ )

$$\begin{pmatrix} \varphi^r \\ \chi^r \end{pmatrix}.$$

In the high-barrier approximation ( $\Delta E_{c,v} \gg |e|V$ ) the components  $\varphi$  and  $\chi$  are given in the region  $|z| < d/2$  by linear combinations of exponentially decaying and growing contributions  $\sim \exp(\pm \kappa z)$ , where the scale of variation of these contributions is determined from (4):

$$\hbar \kappa \approx (\Delta E_c \Delta E_v)^{1/2} / s. \quad (6)$$

We now use the conditions that the  $\varphi$ - and  $\chi$ -components be continuous at  $z = \pm d/2$  [these conditions follow directly from Eq. (4)] and match the coefficients standing in front of the functions  $\exp(\pm \kappa z)$ . As a result we obtain the boundary conditions which connect the  $l$ - and  $r$ -solutions in the narrow-gap materials:

$$\begin{pmatrix} \varphi^r \\ \chi^r \end{pmatrix}_{z=d/2} = \hat{M}_d \begin{pmatrix} \varphi^l \\ \chi^l \end{pmatrix}_{z=-d/2}, \quad \hat{M}_d = \begin{vmatrix} \text{ch } \kappa d & -\alpha^{-1} \text{sh } \kappa d \\ -\alpha \text{sh } \kappa d & \text{ch } \kappa d \end{vmatrix}. \quad (7)$$

The wave functions in the narrow-gap materials are given by the expressions

$$\begin{pmatrix} \varphi_{+i} \\ \chi_{+i} \end{pmatrix} \exp(ik_i z) + \begin{pmatrix} \varphi_{-i} \\ \chi_{-i} \end{pmatrix} \exp(-ik_i z), \quad i=l, r, \quad (8)$$

in which the wave vectors  $k_{l,r}$  are determined from the dispersion relation

$$(\varepsilon_c^j - E)(\varepsilon_v^j - E) = (sp)^2 + (\hbar k_i)^2, \quad i=l, r, \quad (9)$$

obtained from the condition that the system (4) have a non-trivial solution (here  $\varepsilon_{c,v}^i$  are the positions of the band extrema on the left for  $i=l$  and on the right for  $i=r$  of the barrier, as shown in the band diagrams Figs. 1b and 1c). The constant coefficients  $\varphi_{\pm}^i$  and  $\chi_{\pm}^i$  must be found from the boundary conditions (7) and the condition of normalization; the current density (5) is expressed in terms of these coefficients using the relation between  $\varphi$  and  $\chi$  from the upper or lower equations of the system (4). As a result, we can express (5) in terms of the coefficients  $\varphi_{\pm}^i$  or  $\chi_{\pm}^i$  using the relations

$$j|_{E,\sigma,p} = \frac{2s^2\hbar k_i}{E - \varepsilon_v^i} (|\varphi_{+}^i|^2 - |\varphi_{-}^i|^2) = \frac{2s^2\hbar k_i}{\varepsilon_c^i - E} (|\chi_{-}^i|^2 - |\chi_{+}^i|^2), \quad (10)$$

where  $i$  takes on values  $l$  or  $r$ , since the current  $j$  does not depend on position.

In order to investigate tunneling for  $V > 0$  we need that solution to (8) which contains only the transmitted ( $T$ ) wave in the  $r$ -region  $z > d/2$  and which contains both the incident ( $I$ ) and reflected ( $R$ ) wave in the  $l$ -region  $z < -d/2$ ; then for  $z < -d/2$  all the coefficients  $\varphi_{\pm}^i$  and  $\chi_{\pm}^i$  will be nonzero, while for  $z > d/2$  only one pair of components ( $\varphi_{+}^r, \chi_{+}^r$  or  $\varphi_{-}^r, \chi_{-}^r$ ) will be nonzero. The process of separating out the  $I, R$ , and  $T$  contributions to Eq. (8) is analogous to that employed in relativistic quantum mechanics,<sup>7</sup> including the fact that the contributions to the current defined by Eqs. (10) change sign as  $E$  passes into the forbidden band.

### 3. CALCULATING THE INTERBAND TRANSMISSION COEFFICIENT AND TUNNELING CURRENT

In investigating the interband tunneling channel it is convenient to define the current  $j > 0$  using the right-hand side of Eq. (10), since we need only retain the transmitted wave in the  $r$ -region; we have shown that the  $T$  contribution is proportional to  $\chi_{+}^r \exp(ik_r z)$ , while  $\chi_{-}^r = 0$ . We can likewise extract the  $I$  and  $R$  contributions in the region  $c < -d/2$  in an analogous fashion. For the case under consideration here we have  $\varepsilon_c^l > E > \varepsilon_c^r$  (see Fig. 1), so that the  $I$  contribution is proportional to  $\exp(-ik_l z)$  and the  $R$  contribution to  $\exp(+ik_l z)$ . For the currents  $j_{I-}, j_{R-}$ , and  $j_{T-}$  we use the expressions

$$j_I = \frac{2s^2\hbar k_l}{\varepsilon_c^l - E} |\chi_{-}^l|^2, \quad j_R = \frac{2s^2\hbar k_l}{\varepsilon_c^l - E} |\chi_{+}^l|^2, \\ j_T = \frac{2s^2\hbar k_r}{E - \varepsilon_c^r} |\chi_{+}^r|^2, \quad (11)$$

which ensure that the law of current conservation  $j_I - j_R = j_T \equiv j$  is fulfilled.

The transmission coefficient  $T_{\rho\sigma}(E)$  (where the incident electron is characterized by energy  $E$ , the spin quantum number  $\sigma$  and the  $2D$ -momentum  $\mathbf{p}$ ) is defined in the usual way in terms of the currents introduced above:

$$T_{\rho\sigma}(E) = \frac{j_T}{j_I} = \frac{k_r}{k_l} \frac{\varepsilon_c^l - E}{E - \varepsilon_c^r} \frac{|\chi_{+}^r|^2}{|\chi_{-}^l|^2}, \quad (12)$$

so that in order to calculate it we must express  $\chi_{+}^r$  in terms

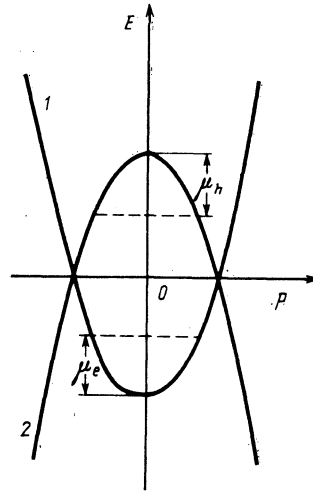


FIG. 2. Dispersion law of narrow-gap materials in the  $r$ - and  $l$ -regions (curves 1 and 2, respectively; the dashed lines correspond to Fermi levels for the cases of  $n$ -type and  $p$ -type doping).

of  $\chi_{-}^l$  using the boundary conditions (7). These algebraic equations are solved directly; however, the results turn out to be quite awkward.<sup>2)</sup> We will limit ourselves to the case of small energy overlap of the conduction and valence bands

$$v \equiv |e|V - \varepsilon_g \ll \varepsilon_g.$$

When low-energy states participate in the interband tunneling process, for (12) we obtain the simple expression

$$T_p(E) \approx \exp(-2\kappa d) \frac{2\hbar^2 k_l k_r}{m\varepsilon_g}. \quad (13)$$

In this case we can also use the parabolic approximation to describe the dispersion law (see Fig. 2)

$$E = \varepsilon_{vl} - \frac{p^2}{2m} - \frac{(\hbar k_l)^2}{2m} = \varepsilon_c^r + \frac{p^2}{2m} + \frac{(\hbar k_r)^2}{2m}, \quad (14)$$

which follows from the dispersion relation (9) in the region of small longitudinal momenta.

The total current  $J$  per unit area is expressed in terms of (12) in the following fashion:

$$J = \int_0^\infty \frac{dk_l}{2\pi} \int \frac{d\mathbf{p}}{(2\pi\hbar)^2} w_l \sum_\sigma T_{\rho\sigma}(E) f_l(1-f_r). \quad (15)$$

Here in place of the variables  $E, \sigma, \mathbf{p}$ , we have used the set  $k_l, \sigma, \mathbf{p}$ , and  $w_l = \hbar^{-1} dE/dk_l$  is the transverse component of the velocity of electrons incident on the barrier; the function  $f_l$  denotes the electron distribution for  $z < -d/2$ , while  $(1-f_r)$  is the distribution of unoccupied states for  $z > d/2$ . In calculating the interband contribution to the tunneling current  $J_{\text{inter}}$  we use the transmission coefficient (13). For either  $n$ - or  $p$ -type materials, the integration in expression (15) is carried out over an energy interval determined by the following inequalities (see Figs. 1 and 2;  $\mu_e$  or  $\mu_h$  are the Fermi energies of the strongly degenerate electrons or holes referenced from the extrema of the corresponding bands):

$$\varepsilon_v^l > E > \varepsilon_c^r + \mu_e \text{ (n-type); } \varepsilon_v^l - \mu_h > E > \varepsilon_c^r \text{ (p-type)}. \quad (16)$$

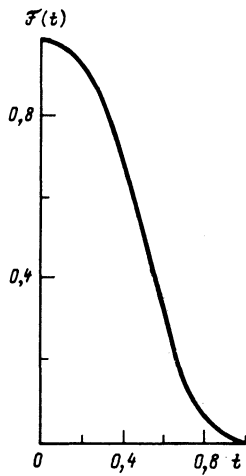


FIG. 3. Plot of the function  $\mathcal{F}(t)$  from (19), which determines the dependence of  $J_{\text{inter}}(v)$  near the threshold for interband tunneling.

In (13) we used the relation obtained from (14)

$$\hbar k_x = [2mv - 2p^2 - (\hbar k_y)^2]^{1/2}, \quad (17)$$

which also limits the region of integration in  $J_{\text{inter}}$ .

For  $v \gg \mu_{e,h}$  only the restriction (17) is important, and we obtain an interband component of the tunneling current which does not depend on the type of doping (the integration is carried out with respect to the longitudinal  $p^2/2m$  and transverse  $\hbar^2 k_y^2/2m$  contributions to the energy measured in units of  $v$ ):

$$\bar{J}_{\text{inter}} = \frac{2m}{3(\pi\hbar)^2} e^{-2\kappa d} \frac{v^3}{\hbar\epsilon_g} \int_0^1 dy y^{1/2} (1-y)^{1/2} = e^{-2\kappa d} \frac{\rho_{2D} v^3}{24\hbar\epsilon_g}, \quad (18)$$

where  $\rho_{2D} = m/\pi\hbar^2$  is the two-dimensional density of states. As the factors  $\mu_{e,h}/v$  vary from zero to one, the interband contribution to the current varies from a maximum value (18) to zero for  $\mu_{e,h} = v$ . Although the limits of integration are different for  $n$ - and  $p$ -type structures [see (16)], this

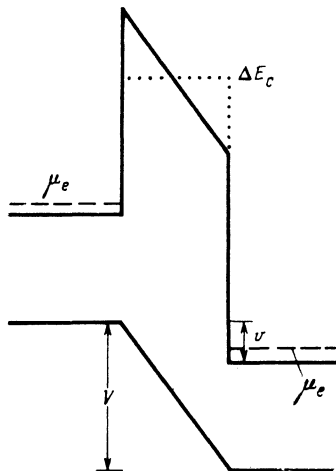


FIG. 4. Band diagram for a heterostructure with  $\Delta E_v = 0$  and  $|e|V > \epsilon_g$  (the notation is the same as in Fig. 1).

limiting behavior does not depend on the type of doping, and the interband contribution is given by the expression

$$J_{\text{inter}} = \bar{J}_{\text{inter}} \mathcal{F}(\mu_e/v) \quad (n\text{-type});$$

$$J_{\text{inter}} = \bar{J}_{\text{inter}} \mathcal{F}(\mu_h/v) \quad (p\text{-type}),$$

$$\mathcal{F}(t) = \frac{2}{\pi} \left\{ \arctg\left(\frac{1-t}{t}\right)^{1/2} + (2t-1)^3 \ln \frac{(1-t)^{1/2} + t^{1/2}}{(|1-2t|)^{1/2}} + 2(1-2t) [(1-t)t]^{1/2} \right\}. \quad (19)$$

The function  $\mathcal{F}(t)$  given in Fig. 3 has the asymptotic form

$$\mathcal{F}(t) \approx 1 - \frac{64}{5\pi} t^{5/2}$$

for small  $t$  and

$$\mathcal{F}(t) \approx \frac{64}{5\pi} (1-t)^{5/2}$$

when its argument is close to unity, so that the singularities at the points  $p = 0, 1/2, \text{ and } 1$  appear only in the third derivative.

Despite our use of a simplified band structure and the approximation of a wide barrier (i.e.,  $E_g = \Delta E_c + \Delta E_v \gg |e|V, \epsilon_g$ ) the expressions given here describe the basic features of interband tunneling. Equation (18) implies a rapid ( $\propto v^3$ ) growth in the pre-exponential factor for voltages larger than  $\epsilon_g + \mu_{e,h}$ , and an exponential decrease in  $\bar{J}_{\text{inter}}$  as the thickness of the barrier increases. In this case the exponent determined by (6) depends on the relative position of the barrier extrema [expressed in terms of  $\alpha = (\Delta E_c/\Delta E_v)^{1/2}$ ]

$$2\kappa d = \frac{\alpha}{1+\alpha^2} \frac{E_g}{[\epsilon_g \epsilon(d)]^{1/2}}, \quad \epsilon(d) = \frac{(\hbar/d)^2}{2m}, \quad (20)$$

so that  $\bar{J}_{\text{inter}}$  turns out to be a minimum for a symmetric barrier (when  $\alpha = 1$ ) and increases with decreasing  $\Delta E_c$  or  $\Delta E_v$ ; this matches the dependence obtained above for  $\Delta E_{c,v} \gg \epsilon_g$ .

#### 4. INTERBAND TUNNELING IN A STRUCTURE WITH $\Delta E_v = 0$

In estimating the maximum increase in (20) due to nonsymmetric positioning of the barrier extrema, we consider only the case of an  $n$ -type tunneling structure with  $\Delta E_v = 0$  (see the band diagram in Fig. 4), which according to the "common anion rule"<sup>8</sup> should apply to the (HgCd)Te-CdTe or PbS-EuS systems. In treating the solution near the barrier, we can replace  $\epsilon_c(z) - E$  in the upper equation in the system (4) by  $E_g$ , so that

$$\varphi \approx -\frac{s}{E_g} \left( \sigma p + \hbar \frac{d}{dz} \right) \chi, \quad (21)$$

when we substitute this expression into the lower equation (4) for  $\chi$  we obtain a second-order equation with a potential energy that depends linearly on the coordinate  $z$ . The solution to this equation is given by linear combinations of Airy functions:

$$\chi = C_1 \text{Ai}(Y) + C_2 \text{Bi}(Y),$$

$$Y = \frac{(E_g |e| V)^{1/2}}{(s\hbar/d)^{3/2}} \left( \frac{z}{d} + \frac{(sp)^2}{E_g |e| V} + \frac{E}{|e| V} \right), \quad (22)$$

At the edges of the barrier  $z = \pm d/2$  the argument  $Y$  in (22) is large, and the boundary condition analogous to (7) which connects the components  $\varphi$  and  $\chi$  on the different sides of the barrier is here expressed in terms of the asymptotic forms of the Airy functions. As a result, the matrix  $\hat{M}_d$  entering into (7) is now given by the following expression, which oscillates with  $d$  and  $V$ :

$$\hat{M}_d = e^{\xi} \begin{vmatrix} \sin\left(\xi + \frac{\pi}{4}\right) & -\gamma^{-1} \cos\left(\xi + \frac{\pi}{4}\right) \\ -\gamma \sin\left(\xi + \frac{\pi}{4}\right) & \cos\left(\xi + \frac{\pi}{4}\right) \end{vmatrix} + \frac{e^{-\xi}}{2} \begin{vmatrix} \cos\left(\xi + \frac{\pi}{4}\right) & \gamma^{-1} \sin\left(\xi + \frac{\pi}{4}\right) \\ \gamma \cos\left(\xi + \frac{\pi}{4}\right) & \sin\left(\xi + \frac{\pi}{4}\right) \end{vmatrix}, \quad (23)$$

in which the following large parameters are introduced:

$$\xi = [ |e| V E_g / \varepsilon_g \varepsilon(d) ]^{1/2} / 3 \cdot 2^{1/2}, \quad (24)$$

$$\gamma = E_g^{3/2} / [ \varepsilon_g \varepsilon(d) ]^{1/2} ( |e| V )^{1/2} \xi^{1/2}.$$

Further calculations involve the use of the wave functions (8), and are analogous to those presented in Secs. 2 and 3. The resulting expressions for the transmission coefficient in the low-energy approximation differ from (13) both by changes in the exponent, which now contains the parameter  $\xi$  introduced in (23), and by the appearance of an additional factor which oscillates as a function of  $\xi$ :

$$T_p(E) \approx \exp(-2\xi) \frac{2\hbar^2 k_l k_r}{m\varepsilon_g} \Psi\left(\frac{p^2}{2mv}, \frac{(\hbar k_l)^2}{2mv}\right)$$

$\Psi(x, y)$

$$= \sum_{\sigma} \left[ \gamma^2 \frac{v}{\varepsilon_g} (x+y) \sin^2\left(\xi + \frac{\pi}{4}\right) - \sigma \gamma \left(\frac{v}{\varepsilon_g} x\right)^{1/2} \cos 2\xi + \cos^2\left(\xi + \frac{\pi}{4}\right) \right]^{-1}. \quad (25)$$

The oscillations of the transmission coefficient arise because when  $z$  is close to  $-d/2$  some motion into the barrier region is allowed for carriers in states of the valence band (see Fig. 4), since the Airy function has an oscillatory rather than a decaying character. Substituting expression (25) into Eq. (15) and integrating with respect to the dimensionless variables  $x$  and  $y$ , we obtain the tunneling current  $J_{\text{inter}}$ , which depends on  $\mu_e/v$  and the parameters  $\xi$  and  $\gamma^2 v/\varepsilon_g$  introduced in (24).

Let us investigate the nature of the oscillatory dependence of  $J_{\text{inter}}$  on  $\xi$  for values of  $\gamma^2 v/\varepsilon_g$  that are small and large compared to unity. For  $\gamma^2 v/\varepsilon_g \ll 1$ , there is a narrow region of values of  $\xi$  close to  $\pi/4 + n\pi$  (where  $n$  is an integer) for which the asymptotic form of the function  $\Psi(x, y)$  is determined by the first term in the denominator of (25), and  $\Psi(x, y) \sim (x+y)^{-1}$ . For the remaining range of variation of  $\xi$  we can use the asymptotic form  $\Psi(x, y) \approx 2/\cos^2(\xi + \pi/4)$ , so that the calculation is analogous to that carried out in Sec. 3, and  $J_{\text{inter}}$  differs from (19)

only by the change in the exponential dependence and the appearance of an oscillatory factor

$$J_{\text{inter}} = e^{-2\xi} \frac{\rho_{2D} v^3}{24\hbar \varepsilon_g} \mathcal{F}(\mu_e/v) / \cos^2\left(\xi + \frac{\pi}{4}\right), \quad \xi \neq \frac{\pi}{4} + n\pi. \quad (26)$$

Let us derive the maximum value of the tunneling current, which cuts off the divergence (26) for  $\xi = \pi/4 + n\pi$ , for the case  $v \gg \mu_e$ , when  $J_{\text{inter}}$  does not depend on the level of doping of the narrow-gap material:

$$J_{\text{inter}}^{(m)} \approx e^{-2\xi} \frac{\rho_{2D} v^3}{\hbar \varepsilon_g} \frac{C}{\gamma^2 v/\varepsilon_g}, \quad \xi \approx \frac{\pi}{4} + n\pi. \quad (26)$$

Here  $C \approx 0.16$  is obtained by numerical evaluation of the integral, which differs from the integral entering into (18) and (19) by an additional factor which comes from the asymptotic form  $\Psi(x, y) \sim (x+y)^{-1}$ .

For  $\gamma^2 v/\varepsilon_g \gg 1$ , the oscillatory dependence of  $J_{\text{inter}}(\xi)$  is shifted by  $\pi/2$  compared to the limiting case described above. Now  $\Psi(x, y)$  is determined by the first term in the denominator (25) everywhere except at the point  $\xi = -\pi/2 + n\pi$ , near which this function can be replaced by a factor of 2. Therefore, at the maximum points (i.e., for  $\xi = -\pi/4 + n\pi$ ) the expression for  $J_{\text{inter}}$  differs from (18) and (19) by the replacement of  $\exp(-2\kappa d)$  by  $\exp(-2\xi)$ , while in the regions between these maximum values we obtain the dependence

$$J_{\text{inter}} = J_{\text{inter}}^{(m)} / \sin^2\left(\xi + \frac{\pi}{4}\right), \quad \xi \neq \frac{\pi}{4} + n\pi, \quad (28)$$

in which we have used the results of the integration during the calculation of (27). The smooth matching of the functions determined by (26) and (28) and cutting off of the divergence of the maximum value (this kind of matching is realized for  $\xi$  close to  $\pm \pi/4 + n\pi$ ) will not be discussed here.

Thus, the growth of  $J_{\text{inter}}$  in the present case  $\Delta E_v = 0$  is determined both by the decrease in the exponential dependence (in place of  $\Delta E_v$  introduced in (16) there now appears  $|e|V/18$ ), and in the oscillatory dependence of the preexponential factor described above, which at the corresponding maximum values of  $\xi$  [the voltages  $V$  at which these maxima are reached are determined by (24)] will also exceed the values introduced into (18).

## 5. THE INTRABAND COMPONENT OF THE TUNNELING CURRENT

In calculating the contribution of the intraband channel to the tunneling current (15), it is necessary to calculate the transmission coefficient for energy intervals which for  $n$ - and  $p$ -type materials are determined by the inequalities (see Fig. 1):

$$\varepsilon_c^l + \mu_e > E > \varepsilon_c^l \quad (n\text{-type}), \quad \varepsilon_v^r > E > \varepsilon_v^r - \mu_h \quad (p\text{-type}). \quad (29)$$

The  $I$ -,  $T$ -, and  $R$ -contributions to the current for these energy intervals are once more identified using relation (10). For  $n$ -type materials the transmitted wave is introduced as in Sec. 3, so that the expression for  $j_T$  coincides with (11), while for the  $j_I$ - and  $j_R$ -currents we obtain

$$j_I = \frac{2s^2\hbar k_l}{E - \varepsilon_c^l} |\chi_{+}^l|^2, \quad j_R = \frac{2s^2\hbar k_l}{E - \varepsilon_c^l} |\chi_{-}^l|^2. \quad (30)$$

For *p*-type material, the transmitted wave is proportional to  $\chi_{-}^r \exp(-ik_r z)$ , and  $\chi_{+}^r = 0$ , so that now the  $j_I$ - and  $j_R$ -currents coincide with expression (11), while for the transmitted current we obtain

$$j_T = \frac{2s^2\hbar k_r}{\varepsilon_c^r - E} |\chi_{-}^r|^2. \quad (31)$$

From these expressions for the currents we obtain the transmission coefficient for the case under discussion according to the relation  $T = j_T/j_I$ . In this case we use the relation between the coefficients  $\chi_{\pm}^{l,r}$  given by the boundary conditions (7). These expressions simplify in the case  $v \ll \varepsilon_g$ . In *n*-type material we use the parabolic dispersion law for the *l*-region and the estimate  $\hbar k_r \approx 2(m\varepsilon_g)^{1/2}$ , while in *p*-type material the parabolic dispersion law describes the *r*-region with  $\hbar k_l \approx 2(m\varepsilon_g)^{1/2}$ . In these approximations we have for  $T$

$$T = e^{-2\alpha d} \frac{4}{(m\varepsilon_g)^{1/2}} \begin{cases} \hbar k_l / (1 + 2\alpha^2) & (n\text{-type}), \\ \hbar k_r / (1 + 2/\alpha^2) & (p\text{-type}), \end{cases} \quad (32)$$

and these expressions differ only by the replacement of  $k_l$  by  $k_r$  and  $\alpha$  by  $\alpha^{-1}$ . These differences can be understood by comparing the band diagrams in Figs. 1b and 1c. Subsequent calculations are carried out in analogy with Sec. 3; however, in *p*-type materials it is convenient to use the variable  $(\hbar k_r)^2/2m$  in integrating. The results for the intraband component

$$J_{\text{intra}} = e^{-2\alpha d} \frac{8\rho_{2D}}{15\pi} \begin{cases} \frac{\mu_e^2}{\hbar} \frac{(2\mu_e/\varepsilon_g)^{1/2}}{1 + 2\alpha^2} & (n\text{-type}), \\ \frac{\mu_h^2}{\hbar} \frac{(2\mu_h/\varepsilon_g)^{1/2}}{1 + 2\alpha^2} & (p\text{-type}) \end{cases} \quad (33)$$

differ in *n*- and *p*-type materials by the replacement of  $\alpha$  by  $\alpha^{-1}$  [as in (32)] and the appearance of Fermi energies for electrons or holes ( $\mu_e$  or  $\mu_h$ ). In contrast to the interband contribution (19), now there is no dependence on  $v$ .

Comparing this contribution with the interband component of the tunneling current gives the expression  $Av^3/\mu_e^{5/2}\varepsilon_g^{1/2}$  for the ratio  $\bar{J}_{\text{inter}}/J_{\text{intra}}$ , where  $A \approx 0.17(1 + 2\alpha^2)$  holds in *n*-type material (in *p*-type material this relation contains  $\alpha^{-2}$  and  $\mu_h$ ). For  $v \gg \mu_{e,h}$ , we can in fact have  $\bar{J}_{\text{inter}}/J_{\text{intra}} \approx 1$ , i.e., where the efficiency of the interband channel is comparable to the intraband channel.

## 6. CONCLUSION

In this section we discuss the approximations used to calculate the tunneling currents (18), (19), (26)–(28), and (33), and also present numerical estimates of the magnitude of  $J_{\text{inter}}$  and the concentration of electron-hole pairs generated at the barrier.

The two-band model introduced by expressions (1), (2) for the heterostructure allows us to consider tunneling between pairs of equivalent valleys in heterostructures based on lead chalcogenides. The isotropic approximation describes PbS, and the results we obtain after summing over the valleys (which increases  $\bar{J}_{\text{inter}}$  by a factor of 4) allow us to

estimate the tunneling current in the PbS–EuS–PbS structure. In this case we have not included the possible mixing of different valleys<sup>3)</sup> by the abrupt (on the scale of a lattice constant) heterostructure potential, nor the contributions of other extrema which would change the character of the below-barrier motion. These approximations have been used previously<sup>4)</sup> in investigating the energy spectrum of optical transitions in superlattices, and agree both with experimental data and with the results of numerical calculations. The model Hamiltonian (1) describes the narrow-gap heterostructure (PbSn)Te with a graded-gap junction [i.e., smooth compared to a lattice constant but abrupt on a scale  $\hbar/(m\varepsilon_g)^{1/2}$ ]. However, the case of a wide-band barrier corresponds to the use of materials in the *l*- and *r*-regions with compositions that are close to gapless. It is also necessary to generalize the calculation we have done for the case of an anisotropic energy spectrum; this, however, is directly carried out by a coordinate transformation which converts an ellipse into a sphere.<sup>11)</sup>

For heterostructures based on the  $A_3B_5$  semiconductors [e.g., InSb–CdTe–InSb or (HgCd)Te] the expressions derived above give only an order-of-magnitude estimate of the tunneling current, since they do not include the complex structure of the valence band.

The case of doped narrow-gap *n*-type or *p*-type materials investigated here (where all the voltage drop occurs at the barrier) is the most convenient one for observing interband tunneling, and is realized in the very-high-dielectric-permittivity structures based on lead chalcogenides. Calculations of the transverse voltage distribution using the Poisson equation will not change the results significantly as long as the band bending near the barrier is small compared to  $\varepsilon_g$ .

The most important limitation on these calculations is the condition  $|e|V \ll \varepsilon_g$ , since even the rather small dependence of the exponent on  $V$  discarded in (20) leads to an appreciable change in the IV characteristics of the tunneling structure. However, when the interband tunneling channel is switched on, the only singularities that appear are in the higher derivatives of the IV characteristics [see the asymptotic form of the function  $\mathcal{F}(t)$  derived in (19)]. Therefore a more detailed calculation of the function  $J_{\text{inter}}(t)$  using the Airy solution analogous to (22) in the barrier<sup>4)</sup> will not yield a more accurate identification of the interband component of the tunneling current.

The study of interband tunneling processes is conveniently carried out not in terms of the IV characteristic, but rather by direct recording of the electron-hole pairs generated at the tunneling barrier for  $V > \mu_{e,h}$ . The switching-on of the interband tunneling channel for  $|e|V > \varepsilon_g$  can be detected by studying the band-to-band luminescence of the nonequilibrium electron-hole pairs when they undergo radiative recombination. The intensity of the luminescence is proportional to the concentration of nonequilibrium pairs  $n(z)$ , which is determined from the continuity equation along with the boundary condition that the tunneling current  $J_{\text{inter}}$  and the diffusion current coincide at the barrier  $z = d/2$ . In the *r*-region  $n(z)$  decays exponentially over a recombination length  $(D\tau_R)^{1/2}$  (where  $D$  is the diffusion coefficient and  $\tau_R$  is the recombination time), and the maximum concentration  $n(d/2)$  is found to equal  $J_{\text{inter}}(\tau_R/D)^{1/2}$ .

Let us turn to numerical estimates for the corresponding chalcogenide structures discussed above,<sup>13</sup> with parameters  $E_g = 1.6$  eV,  $\varepsilon_g \approx 0.25$  eV,  $m = 0.08m_e$ , and values of  $\alpha$  close to unity. For  $d = 25$  Å, a carrier concentration greater than  $10^{18}$  cm<sup>-3</sup>, and  $v \approx 0.15\varepsilon_g$ , we obtain  $J_{\text{inter}} \approx 10^{20}$  cm<sup>-2</sup>·sec<sup>-1</sup> (i.e., the density of electric current due to the interband tunneling channel can reach 10 A/cm<sup>2</sup>). In investigating the case  $\Delta E_v = 0$  or structures based on narrower-gap materials, we find that the current increases by two to three orders of magnitude. For  $D \approx 200$  cm<sup>2</sup>/sec and  $\tau_R \sim 10^{-6}$  sec, the maximum pair concentration  $n(d/2)$  reaches  $2 \cdot 10^{16}$  cm<sup>-3</sup>, so that in these structures we may expect rather intense luminescence.

Let us note that at frequencies close to the fundamental absorption edge (in the region of the Moss-Burstein shift), we may also encounter the case of a negative absorption coefficient. For the parameters given above, negative absorption coefficients for propagation along the plane of the tunneling contact of a waveguide mode can reach  $5 \cdot 10^2$  cm<sup>-1</sup>, which significantly exceeds free-carrier absorption in this spectral region (by at least an order of magnitude). These estimates (which do not include details regarding the mechanisms for pair recombination and absorption of IR radiation by free carriers, nor the structure of the waveguide mode) demonstrate not only the possibility of implementing a rather effective IR radiator, but also that a regime of stimulated emission may be achievable (which would allow us to create an IR laser based on a tunneling structure with only *n*-type or *p*-type materials, i.e., which does not require a *p-n* junction).

<sup>1)</sup> Ref. 3 contains a discussion of tunneling accompanied by mixing of the heavy- and light-hole states. This situation is analogous to the single-band case, because no change occurs in the direction of the current as happens in a transition between electron and hole states (see the discussion in Secs. 2 and 3).

<sup>2)</sup> We note the dependence in (12) on the spin quantum number [which is

unimportant for transitions between low-energy states described by (13)] so that in the case of an anisotropic distribution of carriers in the plane of the barrier (caused, e.g., by current flowing in the plane of the structure) the electron-hole pairs generated by interband tunneling will be oriented with respect to spin.

<sup>3)</sup> Such a process is analogous to intervalley scattering at a surface or crystal-crystal boundary.<sup>9</sup> In order to describe it, we must use boundary conditions for the current that mix the different valleys (this type of boundary condition describes the small mixing of the  $\Gamma$ - and  $X$ -valleys for GaAs-AlAs heterostructures<sup>10</sup>). The intra- and interband contributions to the intervalley current differ only slightly (for symmetrically-placed valleys) and taking these processes into account leads only to a small increase in the currents  $J_{\text{inter}}$  and  $J_{\text{intra}}$ .

<sup>4)</sup> The use of exact solutions is necessary for structures with two tunneling barriers, where the switching-on of the interband tunneling channel between the interbarrier layer of narrow-gap material can lead to an *N*-shaped IV characteristic (see the recent measurements on an InAs-AlSb-GaSb-AlSb-InAs structure<sup>12</sup>).

<sup>1)</sup> E. Burstein and S. Lundqvist, *Tunneling Phenomena in Solids*, Plenum, New York, 1969 (Mir, Moscow, 1973).

<sup>2)</sup> Proc. Vith Intl. Conf. on "Hot Carriers in Semiconductors", Solid-State Electronics **32**, No. 12 (1990).

<sup>3)</sup> J.-B. Xia, Phys. Rev. B **38**, 8365 (1988).

<sup>4)</sup> M. Kriechbaum *et al.*, Superlatt. and Microstruct. **5**, 93 (1989); I. V. Kolesnikov *et al.*, Fiz. Tekh. Poluprovodn. **23**, 954 (1989) [Sov. Phys. Semicond. **23**, 598 (1989)].

<sup>5)</sup> D. Bohm, *Quantum Theory*, Prentice-Hall, New York, 1951 (Fizmatgiz, Moscow, 1961).

<sup>6)</sup> M. de Dios Leyva *et al.*, Phys. Status Solidi (b) **125**, 221 (1984).

<sup>7)</sup> A. Sommerfeld, *Atomic Structure and Spectra*, Vol. 2, Ch. 4. Gostekhizdat, Moscow, 1956 (Atombau und Spektrallinien, Vilweg, Braunschweig, 1939).

<sup>8)</sup> L. L. Chang and K. Ploog (Eds.), *Molecular-Beam Epitaxy and Heterostructures*, NATO Advanced Study Inst., Nijhoff, Groningen, 1985 (Mir, Moscow, 1989).

<sup>9)</sup> V. F. Gantmakher and I. B. Levinson, *Carrier Scattering in Metals and Semiconductors*, North-Holland, Amsterdam, 1987 (Nauka, Moscow, 1984).

<sup>10)</sup> H. C. Liu, Appl. Phys. Lett. **55**, 1019 (1987).

<sup>11)</sup> A. G. Aronov and G. E. Pikus, Zh. Eksp. Teor. Fiz. **51**, 281 (1966) [Sov. Phys. JETP **24**, 188 (1967)].

<sup>12)</sup> J. R. Sonderstrom *et al.*, Appl. Phys. Lett. **55**, 1094 (1989); L. F. Luo *et al.*, Appl. Phys. Lett. **55**, 2023 (1989).

<sup>13)</sup> Yu. I. Ravich, B. A. Efimov, and I. A. Smirnov, *Semiconducting Lead Chalcogenides*, Plenum, New York, 1970 (Nauka, Moscow, 1968).

Translated by Frank J. Crowne